Toll-like receptor 7 regulates pancreatic carcinogenesis in mice and humans

Atsuo Ochi,[1] Christopher S. Graffeo,[2] Constantinos P. Zambirinis,[1] Adeel Rehman,[1] Michael Hackman,[2] Nina Fallon,[1] Rocky M. Barilla,[1] Justin R. Henning,[1] Mohsin Jamal,[1] Raghavendra Rao,[1] Stephanie Greco,[1] Michael Deutsch,[1] Marco V. Medina-Zea,[1] Usama Bin Saeed,[1] Melvin O. Ego-Osuala,[1] Cristina Hajdu,[3] and George Miller[1,2]

[1]Department of Surgery, [2]Department of Cell Biology, and [3]Department of Pathology, S. Arthur Localio Laboratory, New York University School of Medicine, New York, New York, USA.

Pancreatic ductal adenocarcinoma is an aggressive cancer that interacts with stromal cells to produce a highly inflammatory tumor microenvironment that promotes tumor growth and invasiveness. The precise interplay between tumor and stroma remains poorly understood. TLRs mediate interactions between environmental stimuli and innate immunity and trigger proinflammatory signaling cascades. Our finding that TLR7 expression is upregulated in both epithelial and stromal compartments in human and murine pancreatic cancer led us to postulate that carcinogenesis is dependent on TLR7 signaling. In a mouse model of pancreatic cancer, TLR7 ligation vigorously accelerated tumor progression and induced loss of expression of PTEN, p16, and cyclin D1 and upregulation of p21, p27, p53, c-Myc, SHPTP1, TGF-β, PPARγ, and cyclin B1. Furthermore, TLR7 ligation induced STAT3 activation and interfaced with Notch as well as canonical NF-κB and MAP kinase pathways, but downregulated expression of Notch target genes. Moreover, blockade of TLR7 protected against carcinogenesis. Since pancreatic tumorigenesis requires stromal expansion, we proposed that TLR7 ligation modulates pancreatic cancer by driving stromal inflammation. Accordingly, we found that mice lacking TLR7 exclusively within their inflammatory cells were protected from neoplasia. These data suggest that targeting TLR7 holds promise for treatment of human pancreatic cancer.

Introduction

Pancreatic ductal adenocarcinoma is the fourth most common cause of cancer death in the United States and is lethal in more than 95% of cases (1). Unlike most adenocarcinomas, pancreatic cancer is overwhelmingly composed of fibroinflammatory stromal elements, interspersed with islands of neoplastic epithelium (2, 3). Evidence suggests that pancreatic tumor stroma directly affects disease progression and outcome, releasing factors into the tumor microenvironment that promote tumor growth and invasiveness, including insulin-like growth factor and platelet-derived growth factor (4–6). Chemotherapy resistance also correlates with the extent of tumor desmoplasia, with the stroma acting as a physical barrier to cytotoxic agents (7). Notwithstanding, activators of the tumor stroma and the precise interplay between the stroma and transformed ductal epithelial cells remain poorly understood (8). Delineation of the regulatory circuitry promoting expansion of the pancreatic cancer stroma and initiating crosstalk with epithelial cells can greatly expand avenues for therapeutic intervention.

Pattern recognition receptors — the most well-described being the TLRs — are expressed on innate immune cells and selected neoplastic tissues (9). TLR ligands include conserved bacterial and viral molecular motifs, denoted pathogen-associated molecular patterns (PAMPs). TLRs are also bound by diverse byproducts of inflammation and cellular injury, denoted damage-associated molecular patterns (DAMPs). As such, TLRs powerfully link environmental stimuli to innate immunity. TLRs transduce NF-κB and MAP kinase signaling cascades, initiating cytokine production and further recruitment of proinflammatory entities, making them potential mediators in the inflammation-cancer paradigm (9, 10).

TLR7 is expressed within endosomal compartments in a variety of leukocytes, and its ligation triggers an inflammatory response (11, 12). TLR7 activation has been proven an effective treatment of several tumors, including basal cell carcinoma, breast cancer, and melanoma (13). Our preliminary investigations in human and murine systems found that normal pancreata do not express TLR7 or contain TLR7 agonists, yet the receptor is highly expressed in both transformed epithelial cells and peritumoral inflammatory cells in pancreatic cancer. Based on these findings, we postulated that TLR7 regulates pancreatic cancer progression. However, we found that TLR7 ligation was not antineoplastic, but markedly protumorigenic, inducing altered expression of numerous genes that regulate tumor progression via signaling mechanisms that we believe to be novel. Simultaneously, TLR7 inhibition potently protected against cancer development. Collectively, these findings implicate TLR7 as potential target for effective treatment of human pancreatic cancer.

Results

Elevated expression of TLR7 in pancreatic cancer. To determine the relevance of TLR7 to pancreatic cancer, we examined expression of TLR7 in the normal murine and human pancreas and in murine and human pancreatic adenocarcinoma. TLR7 expression was rare in the normal mouse pancreas. Conversely, in pancreata from 6-month-old p48Cre;Kras^{G12D} mice, both inflammatory cells within the tumor microenvironment and ductal epithelial cells robustly expressed TLR7 (Figure 1A). We also found high expression of TLR7 in transgenic mouse models of pancreatic cancer harboring

Authorship note: Atsuo Ochi and Christopher S. Graffeo contributed equally to this work.

Conflict of interest: The authors have declared that no conflict of interest exists.

Citation for this article: *J Clin Invest.* 2012;122(11):4118–4129. doi:10.1172/JCI63606.

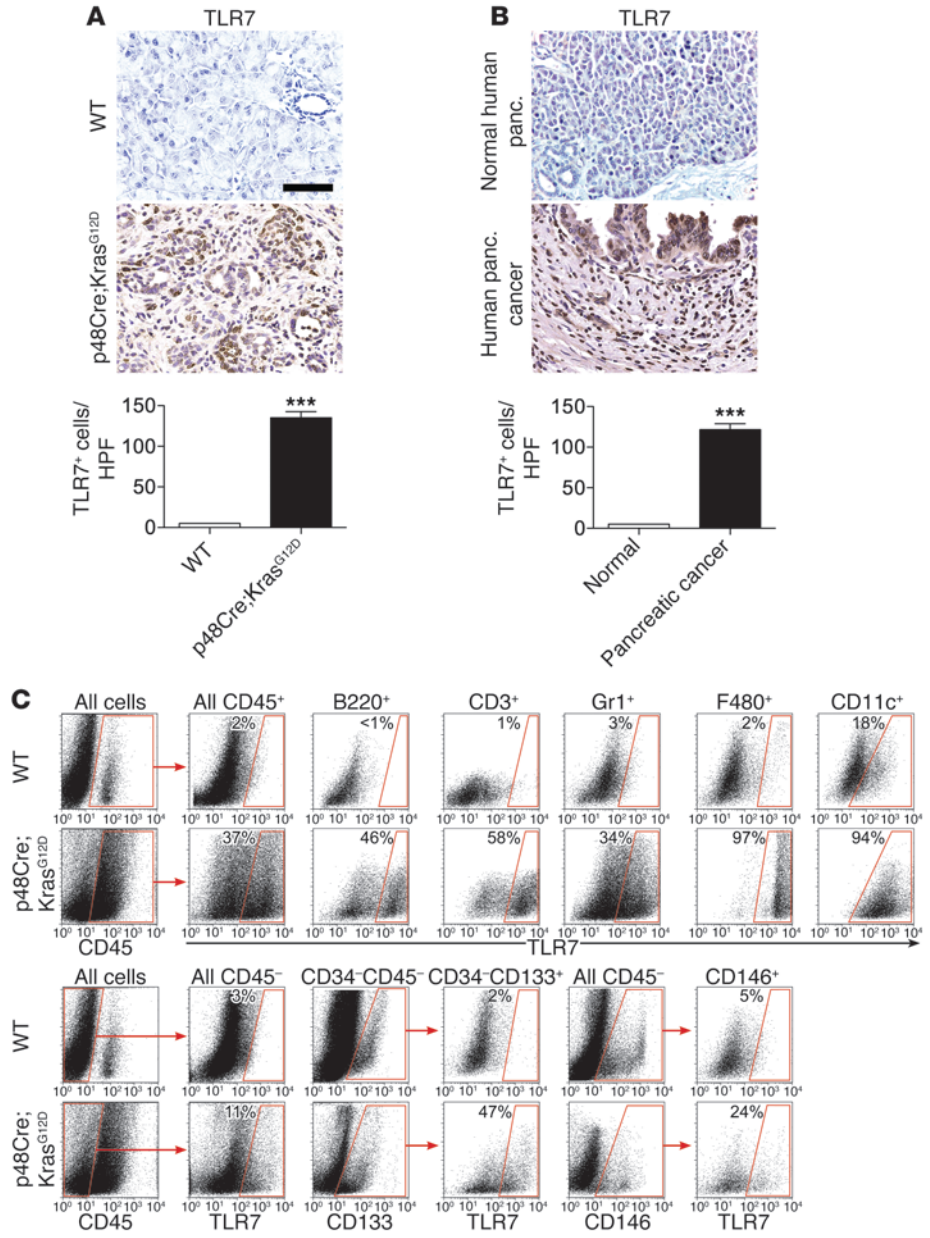

Figure 1

High expression of TLR7 in inflammatory and epithelial cells in pancreatic carcinoma. (**A**) Representative paraffin-embedded sections of pancreata from 6-month-old WT or p48Cre;Kras^{G12D} mice. The number of TLR7$^+$ cells per HPF was quantified (n = 6 per group). (**B**) Human normal (n = 5) and pancreatic cancer (n = 19) paraffin-embedded specimens were stained with mAbs directed against TLR7, and the number of TLR7$^+$ cells per HPF was quantified. (**C**) Pancreatic leukocyte (CD45$^+$) and (**D**) parenchymal (CD45$^-$) cellular subsets from 6-month-old WT and p48Cre;Kras^{G12D} mice were analyzed by flow cytometry for expression of TLR7. The percentage of cells expressing TLR7 for each cellular subset is indicated. Data are representative of experiments repeated more than 3 times. Original magnification, ×40. Scale bar: 75 μm. ***P < 0.001.

additional *Trp53* mutations or Ink4a/Arf deficiency (Supplemental Figure 1A; supplemental material available online with this article; doi:10.1172/JCI63606DS1). Similarly, normal human pancreata did not express TLR7, whereas human pancreatic cancer specimens exhibited high expression of TLR7 in both neoplastic ductal epithelial cells and inflammatory cells within the tumor microenvironment (Figure 1B). Our human tissue microarray revealed uniformly high expression of TLR7 in established pancreatic cancers, but lower levels of expression in patients with preinvasive PanIN lesions. Furthermore, the absence of staining in normal pancreatic tissues suggests increased TLR7 expression with progressive tumorigenesis (Supplemental Figure 1B). Overall, nearly 50% of cells in invasive human pancreatic cancer expressed TLR7. In contrast to TLR7 expression, TLR2 was not highly expressed in murine and human pancreatic cancer (Supplemental Figure 1, C and D).

To investigate which specific parenchymal and stromal cellular subsets gained TLR7 expression in pancreatic cancer, single-cell suspensions were isolated from normal and tumorous mouse pancreata and analyzed for TLR7 expression in CD45$^+$ and CD45$^-$ populations. Whereas leukocytes harvested from normal pancreata expressed minimal TLR7, roughly 50% of B cells, 65% of T cells, 40% of neutrophils, and nearly all macrophages and dendritic cells harvested from tumorous pancreata expressed TLR7 (Figure 1C). To determine whether pancreatic epithelial cells or endothelial cells also gain TLR7 expression in pancreatic cancer, we gated separately on CD34$^-$CD45$^-$ CD133$^+$ epithelial cells (14) and CD45$^-$CD146$^+$ endothelial cells (ref. 15 and Supplemental Figure 2). Consistent with our immunohistochemical observations, roughly 50% of *Kras*-transformed epithelial cells gained TLR7 expression, while only a small fraction of endothelial cells expressed TLR7 in pancreatic cancer (Figure 1D).

TLR7 ligation accelerates pancreatic cancer progression. As TLR7 is highly expressed in pancreatic cancer, we postulated that its ligation can modulate tumorigenesis. To test this, we treated 6-week-old p48Cre;Kras^{G12D} mice with the TLR7 ligand ssRNA40 or saline. Ligation of TLR7 induced vigorous tumor growth (Supplemental Figure 3, A and B). Furthermore, whereas saline-treated p48Cre;Kras^{G12D} mice had residually normal pancreatic architecture, mice exposed to exogenous ssRNA40 exhibited complete effacement of their pancreatic acini, with diffuse PanIN lesions embedded in a dense bed of fibroinflammatory stroma (Figure 2, A–D). *Kras*-transformed ductal epithelial cells

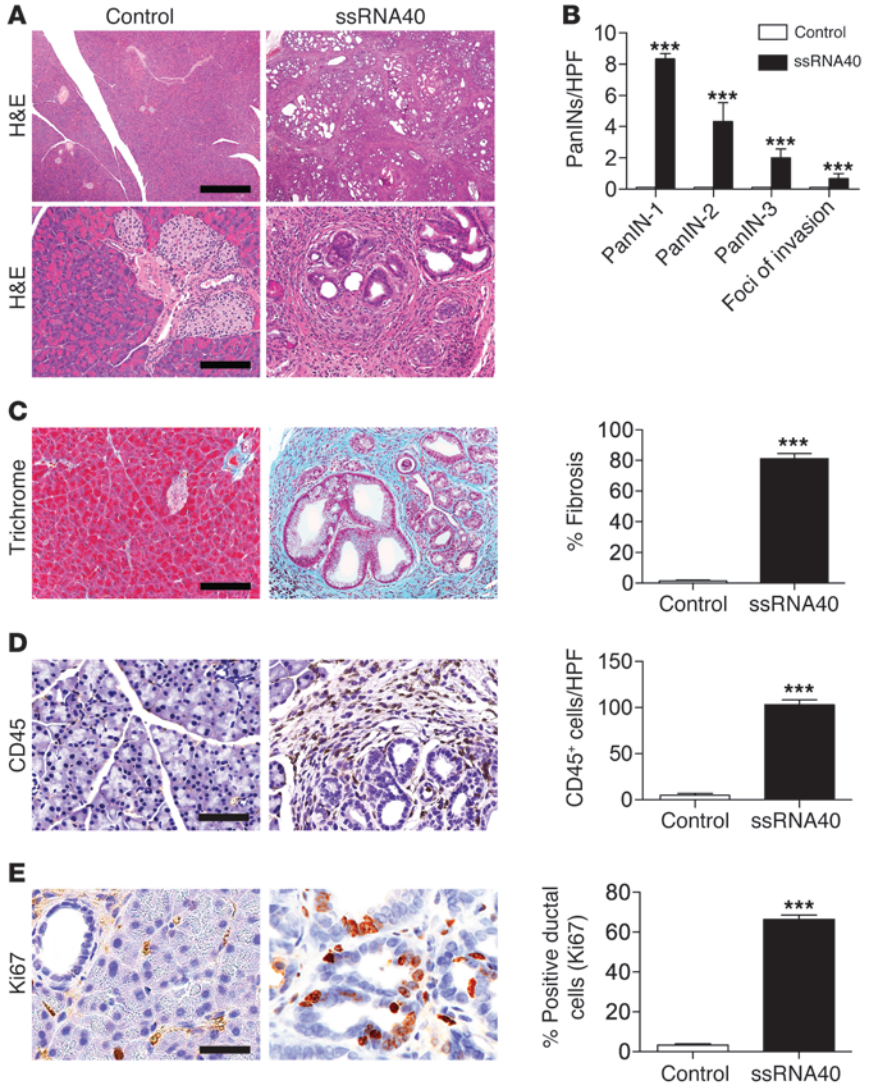

Figure 2

TLR7 ligation accelerates pancreatic tumorigenesis. 6-week-old p48Cre;Kras^{G12D} mice were administered saline or the TLR7 ligand ssRNA40 for 3 weeks. (**A**) Paraffin-embedded sections were examined by H&E. Original magnification, ×4 (top); ×20 (bottom). Scale bars: 700 μm (top); 150 μm (bottom). (**B**) The fractions of various grades of PanINs and foci of invasive cancer were quantified. (**C**) Gimori's trichrome was performed to assess stromal fibrosis. Original magnification, ×20. Scale bar: 150 μm. (**D**) CD45 staining was performed to determine leukocytic infiltration. Original magnification, ×40. Scale bar: 75 μm. (**E**) Ki67 expression, a marker of proliferative index, was tested, and the percentage of Ki67$^+$ ductal cells was determined by examining 10 HPFs per pancreas. Original magnification, ×80. Scale bar: 38 μm. n = 8 per group. ***P < 0.001.

in ssRNA40-treated mice exhibited markedly high Ki67 proliferative rates (Figure 2E) and developed foci of invasive carcinoma (Supplemental Figure 3C). Furthermore, consistent with their more advanced carcinogenesis, treatment of 6-week-old p48Cre;Kras^{G12D} mice with ssRNA40 increased pancreatic epithelial and inflammatory cell expression of TLR7 (Supplemental Figure 3D). Conversely, in accordance with the low expression of TLR2 in pancreatic cancer, treatment of p48Cre;Kras^{G12D} mice with the TLR2 ligand HKLM did not accelerate tumorigenesis (Supplemental Figure 3E).

To determine the effects of TLR7 ligation on molecular pancreatic oncogenesis, we investigated expression of selected cell cycle regulatory and tumor suppressor genes after TLR7 activation. Epithelial cells in ssRNA40-treated p48Cre;Kras^{G12D} mice exhibited a gain of nuclear p53 expression and a selective loss of nuclear p16 expression (Figure 3, A and B, and Supplemental Figure 4). Furthermore, we found a robust gain in expression of p21, p27, p-p27, retinoblastoma protein (Rb), and the SHPTP1 protein tyrosine phosphatase in ssRNA40-stimulated p48Cre;Kras^{G12D} pancreata (Figure 3B). Flow cytometry analysis confirmed elevated epithelial cell expression of p27 and SHPTP1 in pancreata of ssRNA40-treated p48Cre;Kras^{G12D} mice (Figure 3C). Additionally, TLR7 ligation resulted in loss of PTEN expression in neoplastic pancreata (Figure 3D). Consistent with loss of PTEN (16), we found markedly increased expression of pAkt and TGF-β in ssRNA40-treated *Kras*-transformed pancreata (Figure 3D). Loss of PTEN and activation of the PI3K/AKT pathway can induce STAT3 signaling (17), a proinflammatory and tumorigenic pathway recently found to be central to pancreatic carcinogenesis (18–20). Accordingly, we found that TLR7 ligation resulted in markedly increased intrapancreatic expression of STAT3 and p-STAT3 along with their associated proproliferative and antiapoptotic genes c-Myc and Bcl-xL (Figure 3D). TLR7 activation also led to downregulation of cyclin D1, implicated in G1 phase control, and upregulation of cyclin B1, involved in the transition from G2 to M phase (Figure 3D). Taken together, these data suggest that TLR7 activation results in an aggressive tumor phenotype with altered expression of numerous oncogenic targets within the pancreas.

TLR7 inhibition is protective against pancreatic cancer. To determine whether TLR7 is essential to accelerated pancreatic carcinogenesis, we treated mice, in parallel, with caerulein alone to accelerate cancer progression (21) or with caerulein plus an oligonucleotide inhibitor of TLR7 (22). As expected, animals treated with caerulein alone developed accelerated epithelial transformation and peritumoral fibroinflammation; conversely, TLR7 blockade prevented malignant progression or stromal expansion (Figure 4, A–D). These data imply that TLR7 ligation is required for progression of pancreatic neoplasia, and that TLR7 blockade holds significant therapeutic promise. Moreover, treatment of 12-month-old p48Cre;Kras^{G12D} mice harboring invasive pancreatic tumors with an oligonucleotide inhibitor of TLR7 for 2 days resulted in markedly downregulated expression p21, p27, p-p27, cyclin B1, CDK4, and p-STAT3 (Supplemental Figure 5), which indicates that

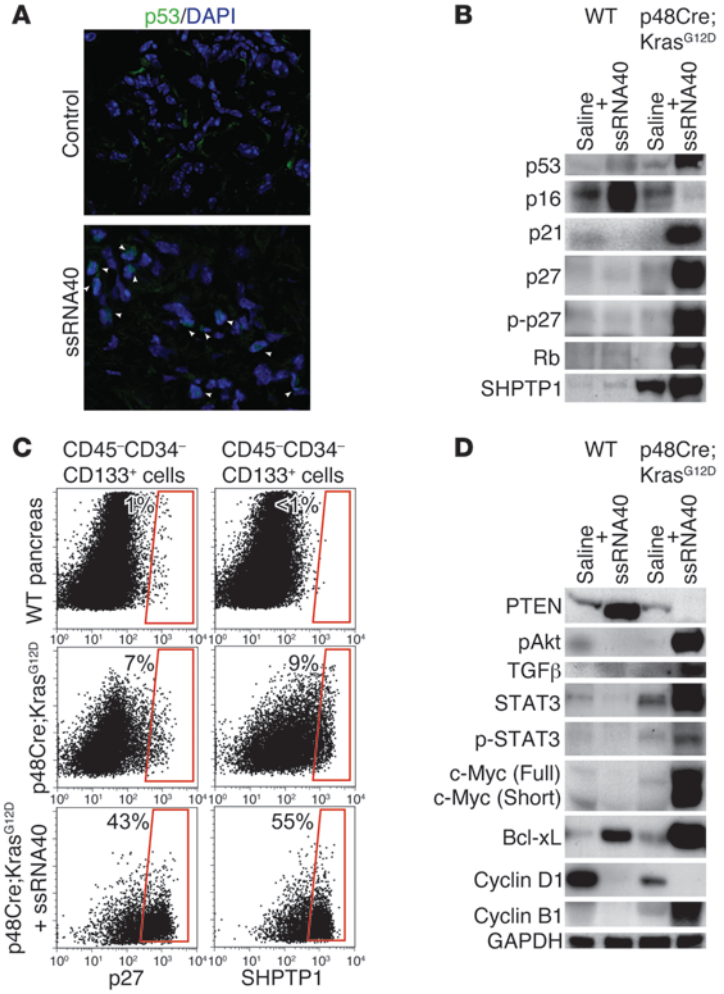

Figure 3

TLR7 activation induces altered expression of tumor suppressor and oncogenic proteins. 6-week-old WT and p48Cre;Kras^{G12D} mice were administered saline or ssRNA40 for 3 weeks. (**A**) Frozen sections of pancreata were stained with DAPI and an mAb directed against p53 and examined for colocalization (arrowheads) by confocal microscopy. Original magnification, ×63. (**B**) Western blots were performed on lysates using mAbs directed against p53, p16, p21, p27, p-p27, Rb, and SHPTP1. (**C**) CD45$^-$CD34$^-$CD133$^+$ pancreatic epithelial cells were gated and analyzed for expression of p27 and SHPTP1 by flow cytometry. The percentage of positively staining cells for each respective marker is indicated. (**D**) Western blots were performed on lysates using antibodies directed against PTEN, pAKT, TGF-β, STAT3, p-STAT3, c-Myc, Bcl-xL, cyclin D1, cyclin B1, and GAPDH. Each Western blot was repeated at least 3 times with similar results.

TLR7 blockade can affect cell cycle regulation in formed pancreatic cancers. Expression of Rb or p53 were not affected by TLR7 inhibition in mice with established tumors (Supplemental Figure 5).

Ligation of TLR7 exacerbates pancreatic inflammation and fibrosis. As expansion of the tumor stroma is critical to pancreatic cancer progression (6), and TLR7 ligation induced vigorous stromal expansion (Figure 2, C and D), we postulated that TLR7 activation exacerbates carcinogenesis by inducing fibroinflammatory stromal growth. Consistent with this hypothesis, we found that in human chronic pancreatitis specimens and in murine models of chronic pancreatitis, a large fraction of infiltrating leukocytes expressed TLR7 (Supplemental Figure 6, A and B). To examine early changes in pancreatic leukocyte expression of TLR7 during inflammation, we used a caerulein model of acute pancreatitis. We discovered a robust recruitment of TLR7-expressing CD4$^+$ and CD8$^+$ T cells, B cells, neutrophils, macrophages, and dendritic cells in acute pancreatitis (Supplemental Figure 6, C and D). Overall, roughly 10%–15% of infiltrating CD45$^+$ leukocytes were TLR7$^+$, with minimal expression in controls. Furthermore, similar to pancreatic cancer, CD34$^-$CD45$^-$CD133$^+$ ductal epithelial cells also increased TLR7 expression in benign pancreatic inflammation, while CD34$^-$CD45$^-$CD146$^+$ endothelial cells did not (Supplemental Figure 6E).

To directly test the effects of TLR7 ligation on fibroinflammatory stromal expansion in the absence of mutated oncogenic *Kras*, we induced chronic pancreatitis in WT mice using either caerulein alone or caerulein plus ssRNA40. In parallel, we treated *Tlr7*$^{-/-}$ animals with caerulein. Ligation of TLR7 markedly increased intrapancreatic inflammation and fibrosis, as well as exocrine and endocrine organ destruction, in WT mice experiencing chronic pancreatitis (Figure 5, A–D, and Supplemental Figure 7, A–C). We also found high periacinar α-SMA expression after TLR7 ligation (Figure 5A), implying activation of pancreatic stellate cells, a central cellular element regulating stromal fibrosis in pancreatic cancer (23). Moreover, *Tlr7*$^{-/-}$ mice were protected in multiple models of pancreatitis (Figure 5, A–D, and Supplemental Figure 7D), which suggests that TLR7 is essential for pancreatic stromal inflammation. However, unlike TLR7-stimulated pancreatic carcinogenesis, there was no evidence of altered expression of cell cycle regulatory genes or tumor suppressor genes in pancreatitis exacerbated by TLR7 activation (Supplemental Figure 7E), which suggests that the molecular changes associated with TLR7-induced carcinogenesis require synergistic epithelial cell expression of oncogenic *Kras*.

To investigate whether intrapancreatic effects of TLR7 activation are specific to ssRNA40 or generalizable to other activating TLR7 ligands, we tested additional well-characterized TLR7 ligands, including *E. coli* ssRNA and adenine analog, which yielded similar effects on pancreatic inflammation (Supplemental Figure 8A) and carcinogenesis (data not shown). To further test the specificity of effects to TLR7 activation, we administered ssRNA40 to *Tlr7*$^{-/-}$ mice. As anticipated, we found no exacerbation of pancreatic inflammation (Supplemental Figure 8B), confirming the specificity of the fibroinflammatory effects. Furthermore, TLR7 agonists had no effects on the pancreas in absence of a baseline level of inflammation (Supplemental Figure 8C). That is, administration of ssRNA40 to mice not experiencing pancreatitis did not induce intrapancreatic stromal expansion (Supplemental Figure 8C), which suggests that the effects of TLR7 on pancreatic fibroinflammation require synergy with preexisting inflammatory elements. To determine whether fibroinflammatory effects of TLR7 ligation were specific to the pancreas, we examined liver, kidney, lung, and intestine from WT mice treated with caerulein and ssRNA40 and found no evidence of disease (Supplemental Figure 9A), which suggests that TLR7 ligation elicits stromal-expansive effects exclusively within the pancreas. Notably, there was minimal TLR7 expression in extrapancreatic organs (Supplemental Figure 9B).

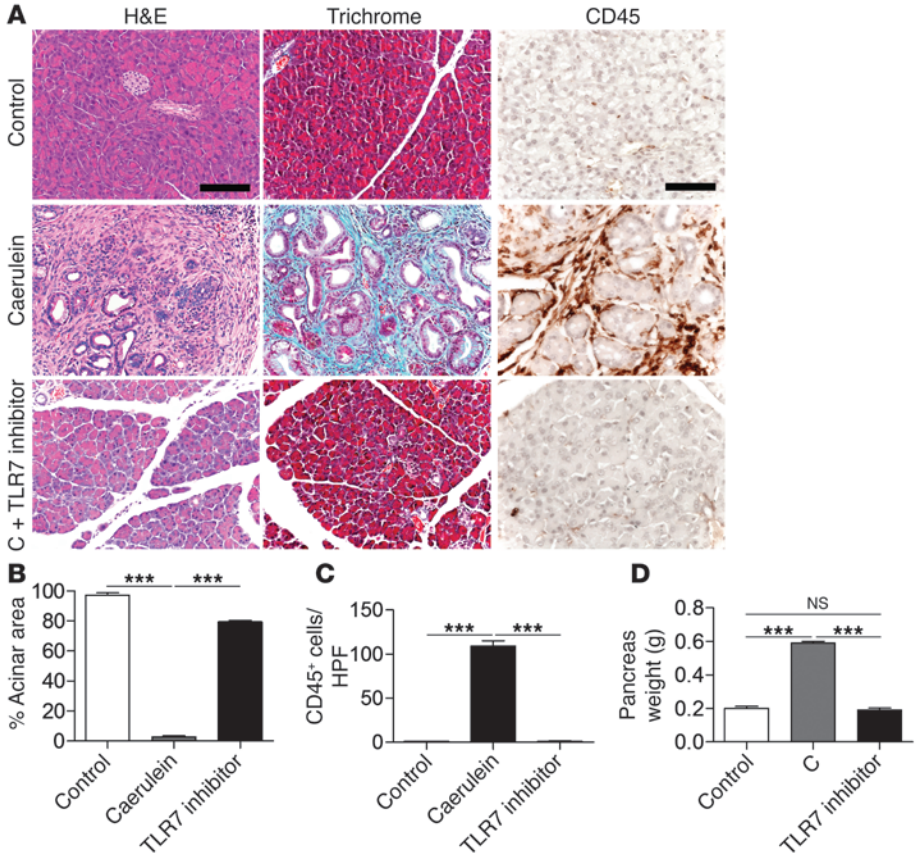

Figure 4

Inhibition of TLR7 protects against pancreatic tumor progression. 6-week-old p48Cre;Kras^{G12D} mice were treated with saline, caerulein (C), or caerulein plus an oligonucleotide inhibitor of TLR7. (**A**) Pancreata were assessed by H&E, trichrome, and CD45 staining. Original magnification, ×20 (H&E and trichrome); ×40 (CD45). Scale bars: 150 μm (H&E and trichrome); 75 μm (CD45). (**B**) Effacement of acini and (**C**) leukocytic infiltrate were quantified by examining 10 HPFs per mouse. (**D**) Whole pancreata were weighed. $n = 8$ per group. ***$P < 0.001$.

Inflammatory cell TLR7 signaling is required for progression of pancreatic carcinoma. We showed that both inflammatory and ductal cells gained expression of TLR7 in pancreatic disease. To directly investigate whether leukocyte or parenchymal cell expression of TLR7 is critical for neoplastic progression, we used *Tlr7*$^{-/-}$ bone marrow chimeric mice, irradiating 2-month-old p48Cre;Kras^{G12D} mice and chimerizing with bone marrow from *Tlr7*$^{-/-}$ mice or WT controls (referred to herein as p48Cre;Kras^{G12D}-*Tlr7*$^{-/-}$ and p48Cre;Kras^{G12D}-WT chimerics, respectively). 7 weeks later, selected cohorts were treated with 2 doses of saline or caerulein to accelerate carcinogenesis; 3 weeks later, mice were sacrificed. The extent of chimerism was greater than 90% (Supplemental Figure 10A). p48Cre;Kras^{G12D}-WT chimerics treated with saline demonstrated metaplastic ducts with scattered early PanINs and exhibited low epithelial cell proliferation rates (Figure 6, A and B). p48Cre;Kras^{G12D}-WT chimerics treated with caerulein developed advanced PanIN lesions with high proliferation rates and scattered foci of invasive cancer (Figure 6, A–C). Remarkably, however, caerulein-treated p48Cre;Kras^{G12D}-*Tlr7*$^{-/-}$ chimerics were protected from accelerated neoplasia (Figure 6, A–C). Moreover, in the absence of caerulein treatment, by 1 year of life p48Cre;Kras^{G12D}-WT chimerics developed frank carcinoma with direct invasion of the stomach and spleen (Figure 6D). However, pancreata in p48Cre;Kras^{G12D}-*Tlr7*$^{-/-}$ chimerics retained residual low-grade metaplastic cysts and early PanINs (Figure 6D). These data indicate that inflammatory cell TLR7 signaling is required for pancreatic cancer progression.

To investigate whether parenchymal cell expression of TLR7 is also important in regulation of pancreatic disease — before treating with caerulein — we made *Tlr7*$^{-/-}$ mice chimeric using WT bone marrow, so that parenchymal cells were deficient in TLR7, whereas inflammatory cells had intact TLR7 signaling. For our 2 control groups, WT mice were made chimeric with WT bone marrow, and WT mice were made chimeric with *Tlr7*$^{-/-}$ bone marrow. We found that WT mice made chimeric with *Tlr7*$^{-/-}$ bone marrow were protected from pancreatic fibroinflammatory disease, as anticipated, whereas pancreata from *Tlr7*$^{-/-}$ mice made chimeric using WT bone marrow were not protected (Supplemental Figure 10B), which suggests that blockade of TLR signaling in pancreatic parenchymal cells does not affect pancreatic inflammation.

To further evaluate any direct proliferative or carcinogenic effects of TLR7 ligation on transformed epithelial cells, we harvested pancreatic ductal epithelial cells (PDECs) from p48Cre;Kras^{G12D} mice and cultured them alone or with ssRNA40. TLR7 ligation had no direct proliferative effects on the transformed epithelial cells (Figure 7A) and did not affect their viability (data not shown). Furthermore, p48Cre;Kras^{G12D} PDEC expression of tumor suppressor or oncogenic genes or genes associated with cell survival and regulation of apoptosis were not altered by TLR7 ligation (Figure 7B). Similarly, treatment of p48Cre;Kras^{G12D} PDECs with ssRNA40 did not increase their proinflammatory cytokine or chemokine production (Supplemental Figure 7C). These data suggest that the carcinogenic changes induced by TLR7 ligation on *Kras*-transformed ductal cells are secondary to direct effects on peritumoral inflammatory cells, rather than being direct effects of TLR7 ligation on epithelial cells.

TLR7 ligation upregulates intrapancreatic Notch, MAP kinase, and NF-κB signaling pathways. The Notch signaling pathway has recently been shown to regulate tumor initiation and maintenance in human and murine pancreatic cancer (24, 25). A recent report indicated that activation of TLRs can directly interface with Notch signaling pathways, resulting in modulation of canonical Notch targets (26); however, the sequential relationship — if any — among TLR ligation, activation of Notch pathways, and pancreatic cancer progression remains unknown. Since mTOR positively regulates Notch signaling via STAT3 (17), and we showed intrapancreatic

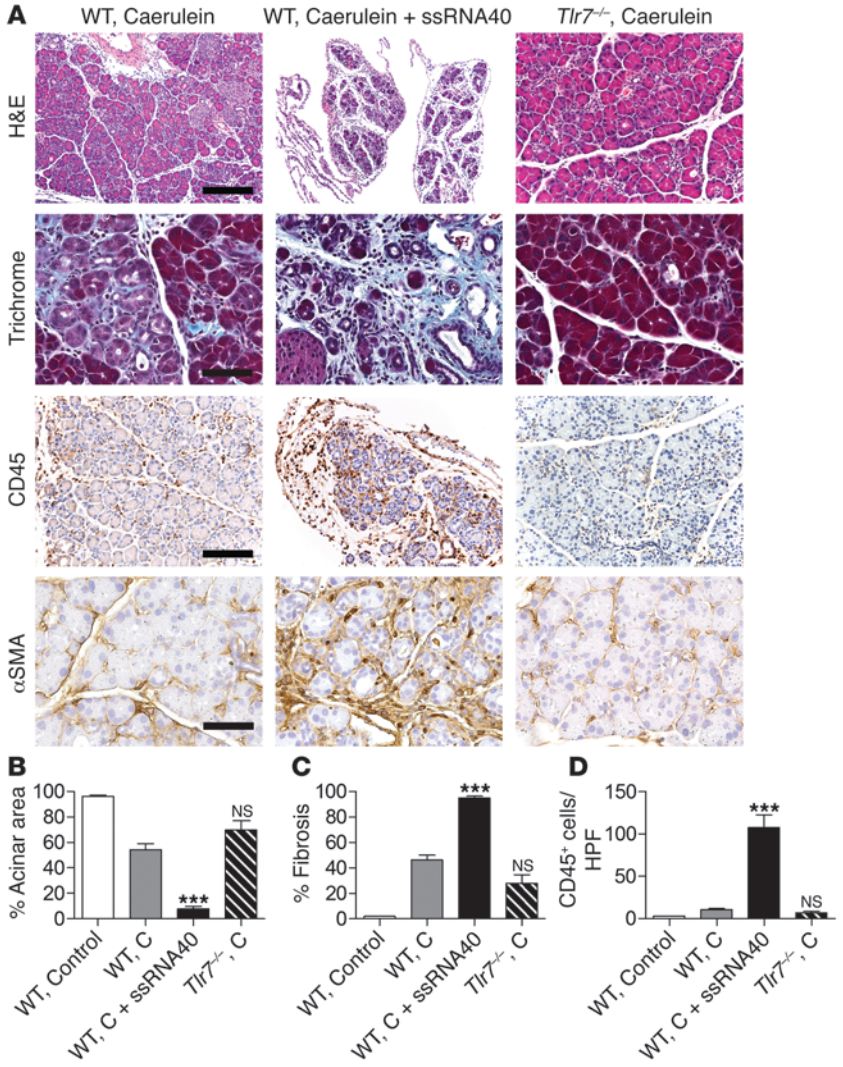

Figure 5

TLR7 ligation exacerbates pancreatic fibroinflammation, while TLR7 inhibition is protective. Chronic pancreatitis was induced in 6-week-old WT or *Tlr7*$^{-/-}$ mice using caerulein. Selected cohorts of WT mice were additionally treated with ssRNA40. (**A**) Pancreata were stained using H&E, trichrome, or mAbs directed against CD45 and α-SMA. Original magnification, ×10 (H&E); ×20 (CD45); ×40 (trichrome and a-SMA). Scale bars: 300 μm (H&E); 150 μm (CD45); 75 μm (trichrome and a-SMA). (**B**) Surface area occupied by acinar units and (**C**) fibrotic surface area were determined using a computerized grid. (**D**) CD45$^+$ leukocytic infiltrate was quantified by examining 10 HPFs per pancreas. $n = 5$ per group. ***$P < 0.001$.

STAT3 activation after TLR7 ligation (Figure 3D), we postulated that TLR7 ligation upregulates Notch signaling mechanisms in the pancreatic tumor microenvironment, thus exacerbating inflammation. We found that p48Cre;Kras^{G12D} pancreata treated with ssRNA40 exhibited increased expression of Notch1 and Notch2 (Supplemental Figure 11, A and B). The Notch ligand Jagged1 was also upregulated in ssRNA40-treated p48Cre;Kras^{G12D} mice (Supplemental Figure 11C). Surprisingly, however, Notch target genes Hes1 and Hey1 were downregulated in p48Cre;Kras^{G12D} pancreata after TLR7 ligation (Supplemental Figure 11C). Consistent with loss of Hes1 (27), we found markedly elevated expression of PPARγ in pancreata of ssRNA40-treated mice (Supplemental Figure 11D). Based on these data, we suspected that TLR7 activation may direct the Notch signaling pathway toward proinflammatory mechanisms, consistent with reports supporting transcriptional activation of NF-κB intermediates by Notch signaling (28). Accordingly, pancreata from 2-month-old p48Cre;Kras^{G12D} mice treated with ssRNA40 expressed high levels of p-IκB and p-Erk1 (Supplemental Figure 11E), indicative of vigorous NF-κB and MAP kinase signaling. To investigate the dependence of TLR7-mediated carcinogenesis on MAP kinase and NF-κB intermediates, we selectively blocked each signaling pathway in p48Cre;Kras^{G12D} mice undergoing TLR7 ligation. MAP kinase and NF-κB blockade both protected against the protumorigenic effects of TLR7 ligation (Supplemental Figure 11F). Blockade of MAP kinase or NF-κB also mitigated the fibroinflammatory effects of ssRNA40 on benign pancreatic disease (Supplemental Figure 12).

Both inflammatory and epithelial cells upregulate NF-κB, MAP kinase, Notch, and STAT3 signaling in TLR7-induced accelerated pancreatic cancer. Whereas TLR7 ligation has no direct effects on epithelial cell viability, proliferation, production of proinflammatory cytokines, or molecular oncogenesis, we found that the critical cell signaling events observed in p48Cre;Kras^{G12D} mice occurred in both inflammatory and epithelial cells. In particular, by gating separately on CD45$^+$ inflammatory cells and CD34$^-$CD45$^-$ CD133$^+$ epithelial cells (Figure 8A), we found that both compartments upregulated expression of Notch1, Jagged1, and Delta4 after TLR7 activation (Figure 8B). Similarly, NF-κB intermediates were upregulated in both the inflammatory and the epithelial compartments (Figure 8C). Furthermore, immunohistochemical analysis revealed markedly increased STAT3 phosphorylation (Figure 8D) and MAP kinase activation (Figure 8E) in both epithelial and inflammatory cells in pancreata of ssRNA40-treated p48Cre;Kras^{G12D} mice compared with saline-treated controls. Taken together, these data imply that whereas the target of direct TLR7 activation — based on experiments using chimeric mice and purified p48Cre;Kras^{G12D} PDECs — is peritumoral inflammatory cells, TLR7-mediated inflammation is sufficient to induce pleiotropic cell signaling changes in the epithelial compartment in the context of oncogenic *Kras*.

Discussion

The urgent need for scientific understanding of pancreatic carcinogenesis is heightened by its clinical futility. Here, we demonstrated that TLR7 expression was markedly increased in pancreatic cancer in mice and humans and showed graduated TLR7 expression in the progression from PanINs to invasive cancer. We showed that ligation of TLR7 dramatically accelerated pancreatic carcinogenesis, while inhibition of TLR7 at several strata — receptor inhibition, receptor deletion, and blockade of downstream signaling

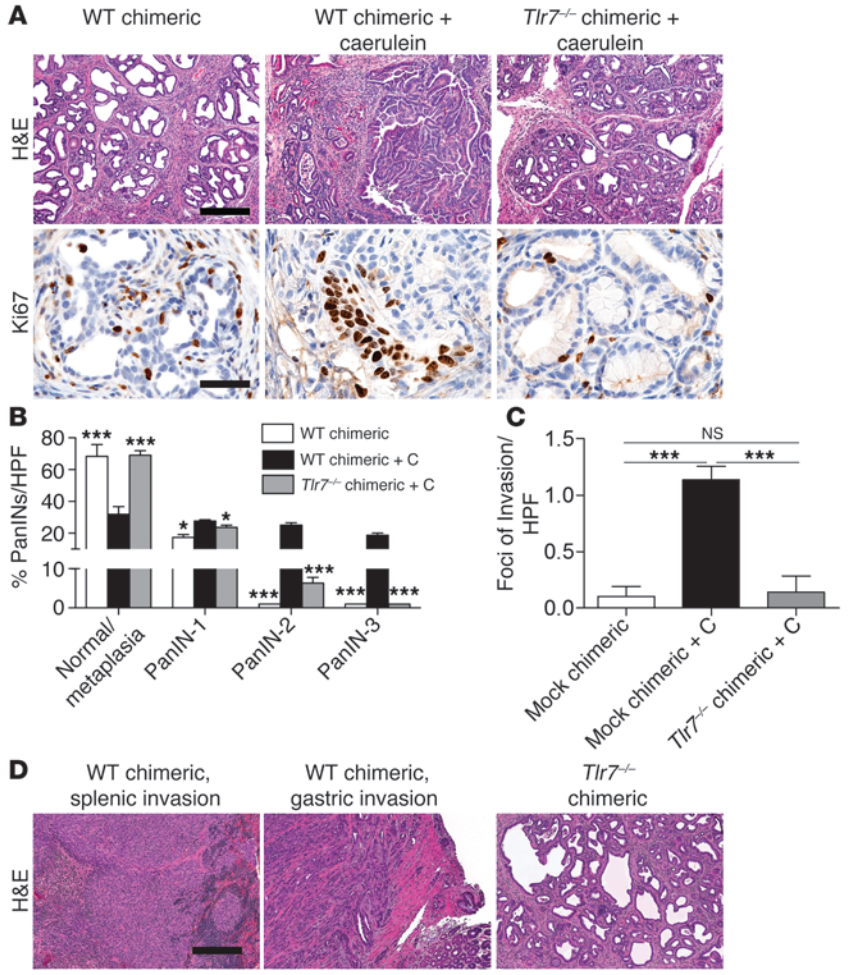

Figure 6

TLR7 signaling in inflammatory cells regulates pancreatic cancer progression. 2-month-old p48Cre;Kras^{G12D} mice were irradiated and made chimeric by bone marrow transfer from WT or *Tlr7*$^{-/-}$ mice. (**A**) 7 weeks later, mice were treated with either saline or caerulein to accelerate carcinogenesis. Mice were then sacrificed 3 weeks later, and pancreata were assessed by H&E and Ki67 staining. Original magnification, ×10 (H&E); ×60 (Ki67). Scale bars: 300 μm (H&E); 50 μm (Ki67). (**B**) The fraction of metaplastic and dysplastic ducts was measured for each cohort, and (**C**) the number of foci of invasive cancer was quantified using CK19 immunohistochemistry (n = 5 per group). *P < 0.05; ***P < 0.001. (**D**) Additional cohorts of chimeric mice (n = 4 per group) were not treated with caerulein, but kept until 12 months of life for histological analysis. Representative H&E-stained paraffin-embedded sections are shown. Original magnification, ×10. Scale bar: 300 μm.

siveness of pancreatic cancer (16). Notably, p16 loss is associated with PanIN lesions at greatest risk for malignant transformation (32, 33). The p16 protein transcriptionally inhibited the Rb tumor suppressor. Accordingly, we found marked Rb overexpression in ssRNA40-treated p48Cre;Kras^{G12D} mice. Rb overexpression has also been demonstrated in human pancreatic ductal adenocarcinomas (32). However, our finding was surprising in light of a recent report showing that deletion of Rb accelerates pancreatic carcinogenesis and impairs senescence in premalignant lesions (34). We further showed that TLR7 ligation led to upregulated expression of p21, p27, and p53, genes whose dysregulation is associated with increased cellular proliferation (35). TLR7 activation also induced downregulation of cyclin D1, which is implicated in G1 phase control, and upregulation of cyclin B1, which is involved in the transition from G2 to M phase. Taken together, our findings indicate that TLR7 activation within the pancreatic tumor microenvironment results in a distinctly aggressive oncogenic phenotype.

Our data provided mechanistic and empirical evidence in support of a sophisticated crosstalk between stromal and epithelial cells driving carcinogenesis. Our chimerization models demonstrated that TLR7 blockade within the inflammatory tumor microenvironment alone was sufficient to halt cancer progression (36, 37). Downstream of TLR7 ligation, we implicated canonical NF-κB and MAP kinase pathways as well as upregulated Notch expression, providing important evidence indicative of a novel TLR-Notch interface that promotes inflammation within the pancreatic tumor microenvironment. Engagement of Notch receptors by Notch ligands — both of which are upregulated in TLR7 — caused a self-amplifying loop that promoted inflammation through the production of proinflammatory cytokines. Our finding that specific Notch target genes, which are critical in organ differentiation, were suppressed in the tumor microenvironment, despite upregulation of Notch ligands and receptors, suggests that Notch signaling may be diverted toward inflammatory end-products in pancreatic carcinoma driven by TLR7 activation. The upregulation of Notch targets, such as the HES-related genes, after Notch receptor upregulation is not universal (38). Furthermore, a multitude of proteins interact with the Notch intracellular domain and activate pathways in parallel, rather than downstream of the traditional Notch-associated transcription factors (38). This is consistent with recent reports suggesting that Notch cooperates with NF-κB signaling (28). Notwithstanding, our findings of simultaneous Notch target gene suppression and PPARγ activation further support the unique inflammatory and oncogenic phenotype associated with TLR7 activation in pancreatic carcinoma. The latter stands in

pathways — rescued animals from pancreatic cancer. TLR7 activation resulted in a distinct oncogenic phenotype in pancreatic carcinoma, with loss of both PTEN and p16 and increased expression of p21, p27, p-p27, p53, Rb, c-Myc, TGF-β, and SHPTP1. Loss of PTEN has previously been reported to accelerate *Kras*^{G12D}-induced pancreatic cancer (29). Consistent with PTEN loss, we found elevated expression of its downstream target, pAkt, which is associated with increased tumor proliferation and enhanced angiogenesis (30). Furthermore, PI3K/Akt signaling has been reported to sustain elevated c-Myc expression, which prognosticates advanced tumor grade and poor survival in human pancreatic cancer (31). Also consistent with PTEN suppression, after TLR7 ligation, we found elevated TGF-β, which is associated with enhanced inva-

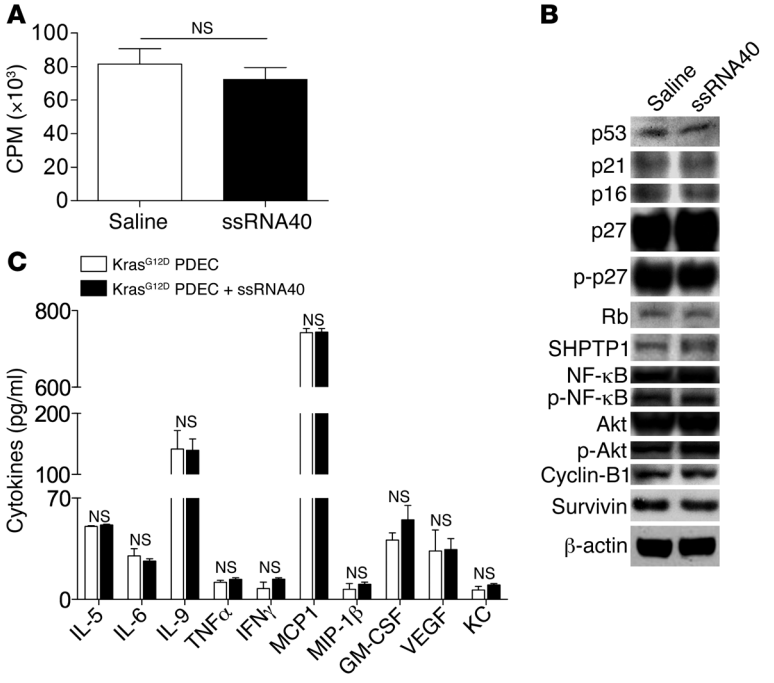

Figure 7

TLR7 ligand does not directly activate PDECs. (**A**) In vitro proliferation of p48Cre;Kras^{G12D} PDECs was measured by uptake of [^{3}H]-thymidine after stimulation with ssRNA40 or saline. (**B**) p48Cre;Kras^{G12D} PDECs treated with ssRNA40 or saline were tested for expression of various tumor-suppressor or oncogenic proteins and for genes involved in regulation of apoptosis by Western blotting. (**C**) Cytokine production by p48Cre;Kras^{G12D} PDECs was measured after stimulation with ssRNA40 or saline. Experiments were repeated 3 times and performed in triplicate.

significant contrast to pancreatic cancers induced by generalized inflammation (for example, via TNF-α administration), which have recently been shown to accelerate tumor progression in association with Hes1 overexpression and PPARγ suppression (27). A central mechanistic element accounting for the intrinsic differences that characterize TLR7-induced inflammatory oncogenesis may be activation of STAT3, which is phosphorylated in the context of PTEN suppression and has been associated with increased Notch signaling and altered expression of the antiapoptotic genes c-Myc and Bcl-xL (17). We expanded on the recent discovery that STAT3 is central to neoplastic progression in pancreatic cancer (18, 19) by demonstrating that TLR7 blockade arrested tumor progression.

Notably, TLR activation in WT mice undergoing pancreatitis, while exacerbating inflammation and inducing NF-κB and MAP kinase activation, did not alter the expression of cell cycle regulatory, oncogenic, or additional proinflammatory genes. This dichotomy suggests that effects observed after TLR7 ligation in p48Cre;Kras^{G12D} mice are specific to pancreatic cancer. Moreover, our findings of important cell signaling and oncogenic changes in neoplastic epithelial cells — despite demonstrating that TLR7 ligands did not directly activate epithelial cells — implicate synergistic interplay between transformed ductal epithelial cells and the activated tumor microenvironment as a result of TLR7 ligation (Figure 9).

We demonstrated, for the first time to our knowledge in any endogenous tumor, that cancer progression could be halted by selective TLR blockade, a finding with important clinical and therapeutic implications. Furthermore, our complementary findings that TLR7 ligation was powerfully protumorigenic and TLR7 blockade arrested pancreatic carcinogenesis contrast sharply with a number of reports in other cancer subtypes that have found TLR agonists — including TLR7 agonists — to be antineoplastic. Experimental models of glioma have shown tumor apoptosis in response to TLR9 and TLR3 ligation. Similarly, TLR3 activation triggers apoptosis in human breast cancer cells, and mouse D2F2 mammary tumors demonstrate inhibited growth following TLR5 ligation (39, 40). Ligation of both TLR7 and TLR9 in CLL directly induces cancer cell death by enhancing activation of cytotoxic NK cells and CD8$^+$ T cells and by promoting the production of antiangiogenic factors (41). Furthermore, several TLR agonists have been tested in clinical trials as antineoplastic agents: the TLR7 agonist imiquimod has been approved as a treatment for basal cell carcinoma, while CYT004-MelQbG10 (another TLR7-specific ligand) has been used to treat advanced melanoma. The TLR3 ligand IPH-31XX has been investigated in patients with breast cancer, and IMOxine and dSLIM9 (both TLR9 agonists) have been tested in renal cell carcinoma and metastatic colorectal cancer, respectively (13). CpG B class ODNs, which signal through TLR9, have been tested in combination chemotherapy regimens in patients with non–small-cell lung cancer and non-Hodgkin lymphoma (42, 43).

The antitumor effects of TLR activation in diverse cancer subtypes are postulated to proceed via several parallel mechanisms, including potentiating innate immune responses via NK cell, monocyte, and macrophage activation; inducing the generation of tumoricidal cytokines; inducing Th1 deviation of CD4$^+$ T cells; augmentation of CTLs; and direct induction of apoptosis in TLR-expressing tumor cells (13). The effects of TLR ligation in clinical cancer therapy are also thought to be amplified in combination with cytotoxic chemotherapy or radiation resulting from the high levels of DAMPs liberated by tumor cell death (44, 45).

While our findings in pancreatic cancer are seemingly in conflict with these reports, the patterns are not necessarily contradictory, as the effects of selective TLR activation in cancer progression may be contingent on the specific roles played by immunity and inflammation in each particular malignancy. In neoplastic processes without an evident primary inflammatory component, TLR ligation may break self-antigen tolerance, promoting antitumor immune responses (46). For example, in *neu* transgenic mice, an attractive model mimicking human Her-2/neu$^+$ breast cancer, TLR7 ligation elicits significant tumor regression by augmenting antitumor immunity (47). However, in neoplastic conditions that arise from inflammation and are driven by continued inflammation, such as pancreatic cancer associated with longstanding pancreatitis, selective TLR ligation may be protumorigenic. Parallel examples are best exemplified by ulcerative colitis–induced colon cancer and *Helicobacter pylori*–associated gastric cancer, diseases governed by a primary inflammatory component with an essential link between the proinflammatory environment initiated by TLR activation (particularly TLR4) and the ensuing malignant degeneration and metastasis (48, 49). The notion that pancreatic cancer similarly arises from inflammatory disease is supported by both experimental obser-

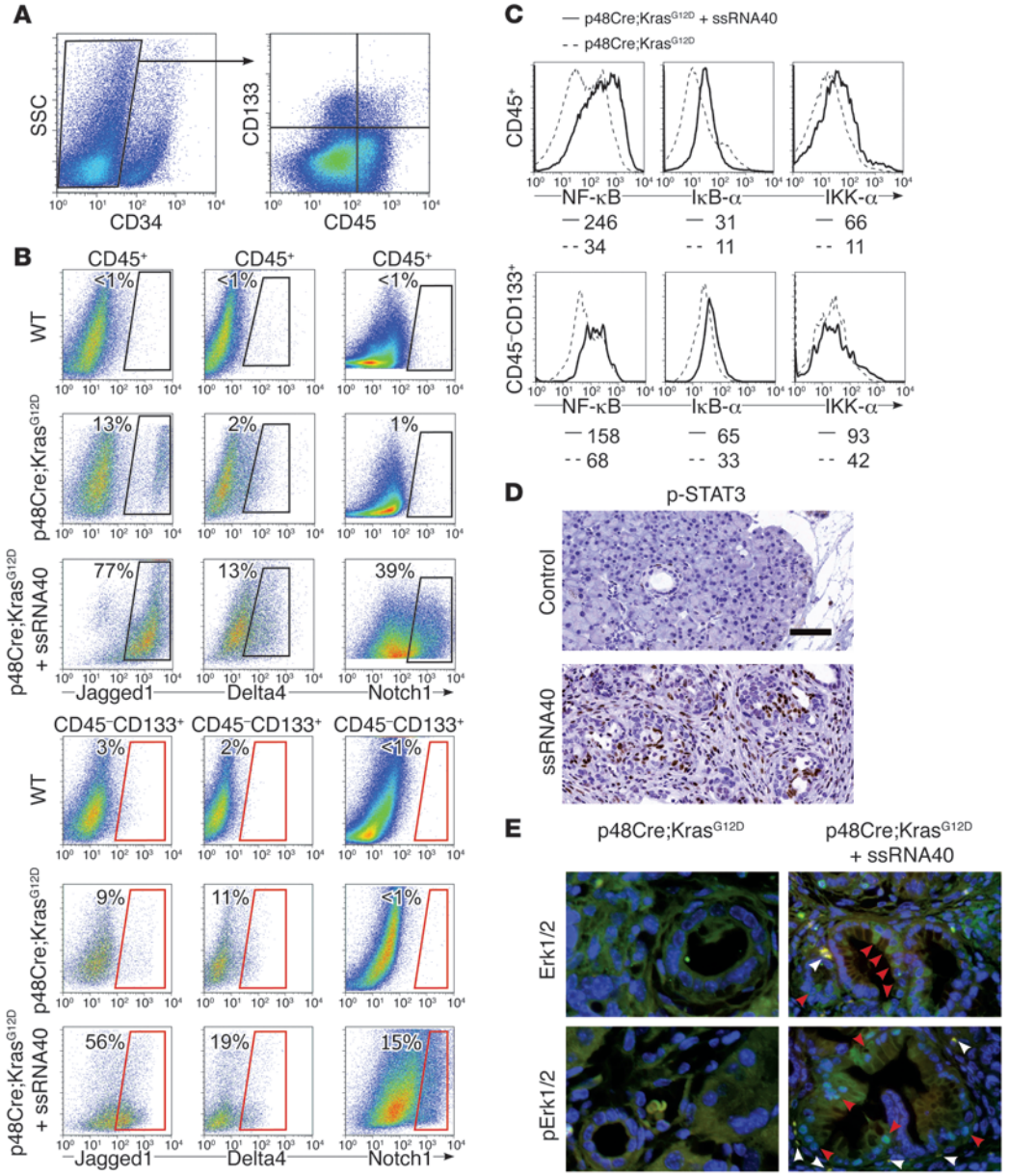

Figure 8

TLR7 activation induces cell signaling changes in both peritumoral inflammatory and ductal epithelial cells in pancreatic cancer. (**A**) To identify epithelial cells, CD34⁻ pancreatic cellular suspensions from p48Cre;Kras^{G12D} mice were gated and costained for CD133 and CD45. (**B**) CD45⁺or CD34⁻CD45⁻CD133⁺ pancreatic cells from 9-week-old WT mice or p48Cre;Kras^{G12D} mice treated with saline or ssRNA40 for 3 weeks were analyzed for expression of Jagged1, Delta4, and Notch1 on flow cytometry. The percentage of positive cells for each respective marker is shown. Experiments were repeated twice using 2–4 mice per group with similar results. (**C**) CD45⁺ or CD34⁻CD45⁻CD133⁺ pancreatic cells from 9-week-old p48Cre;Kras^{G12D} mice treated with saline or ssRNA40 were also analyzed for expression of NF-κB signaling intermediates. MFI is indicated. (**D**) Paraffin-embedded sections of saline and ssRNA40-treated p48Cre;Kras^{G12D} mice were stained for p-STAT3. Representative images are shown. Original magnification, ×40. Scale bar: 75 μm. (**E**) Frozen sections of saline- and ssRNA40-treated p48Cre;Kras^{G12D} mice were stained for DAPI and Erk1/2 or pErk1/2. Localization of Erk1/2 or pErk1/2 in inflammatory cells (white arrowhead) and ductal epithelial cells (red arrowhead) is indicated. Representative images are shown. Original magnification, ×40. Experiments were repeated twice.

vations and clinical evidence: chronic pancreatitis patients have an 8-fold increased risk of pancreatic cancer, and familial pancreatitis is associated with a 40%–75% lifetime risk of neoplasia (50, 51). Recent evidence further suggests that TLR7 activation may stimulate tumor development in colon cancer and lung cancer by promoting inflammation and tumor cell survival (52, 53).

Emerging evidence suggests that the pancreatic tumor microenvironment is rife with DAMPs (54–56). While our data imply that DAMPs released in the tumor microenvironment drive tumorigenesis by stimulating TLR7, it is noteworthy to consider the fact that the natural ligands for TLR7 are viral byproducts (57), which suggests that our data may have implications for theories of virally

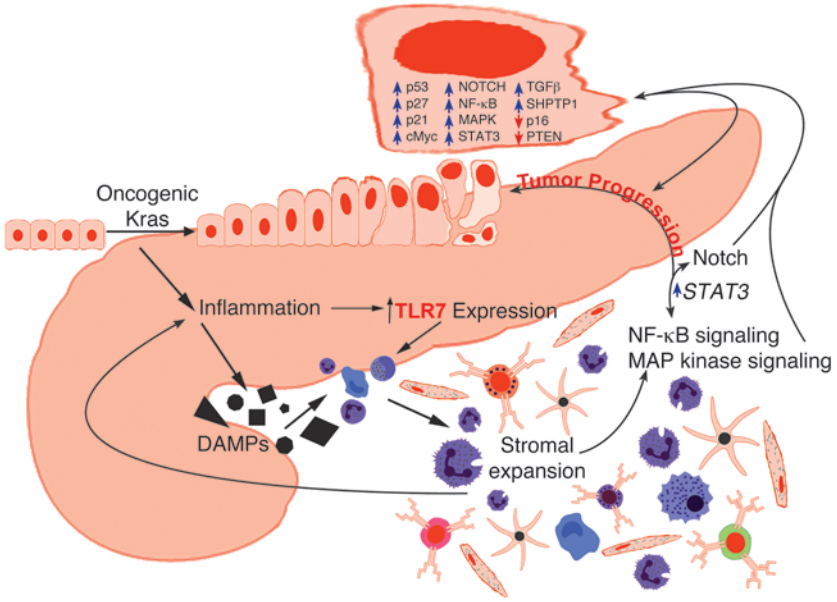

Figure 9
Schematic depicting central position of TLR7 regulation of pancreatic tumorigenesis.

induced etiologies of pancreatic carcinogenesis (58, 59). HCV transmits its genome as ssRNA and can induce chronic fibroinflammatory disease in the liver, which progresses to hepatocellular carcinoma in 2%–6% of carriers (60, 61). Moreover, a cohort study of 146,394 HCV-infected and 572,293 non–HCV-infected US military veterans demonstrated a significant association between systemic HCV infection and pancreatic cancer, independent of liver cancer development (62). Other studies established correlations between HBV or TT virus (TTV) infection and pancreatic cancer (58, 59). Significantly, ongoing HBV infection in the absence of the anti-HBs antibody correlates with a higher risk of pancreatic cancer compared with anti-HBs$^+$ patients who recovered from HBV infection, supporting a role for viral infection in the pathogenesis of this malignancy. Thus, our discoveries surrounding the regulatory role of TLR7 in pancreatic tumorigenesis provide mechanistic support for the expanding empiric link between viral infection and pancreatic cancer.

Our data suggest that TLR7 is a principal modulator of the tumor microenvironment, driving neoplastic progression (Figure 9). Timely translation of these results to a phase I/II clinical trial is indicated to improve the bleak landscape for patients with pancreatic cancer. Clinical-grade TLR7 inhibitors have been successfully tested in systemic lupus erythematosus, a pernicious inflammatory disease (22). Using TLR7 inhibition in human pancreatic cancer — either alone or in combination with standard chemotherapy regimens — may offer hope for improved survival in patients suffering from pancreatic carcinoma.

Methods

Animals and cancer model. C57BL/6 (H-2Kb) mice, CD45.1 (B6.SJL-*Ptprc*^{a} *Pep3*^{b}/BoyJ) mice, and mice deficient in TLR7 (B6.129S1-*Tlr7*^{tm1Flv}/J) or NF-κB (B6.129P-*Nfkb*^{tmBal}/J) were purchased from Jackson Labs. p48Cre;Kras^{G12D} mice, which develop pancreatic neoplasia endogenously by expressing a single mutant *Kras* allele in progenitor cells of the pancreas (gift of D. Bar-Sagi, New York University, New York, New York, USA), were generated by crossing LSL-Kras^{G12D} mice with p48Cre mice, which express *Cre* recombinase from a pancreatic progenitor-specific promoter (63). Tissue from KPC (KrasLSL.G12D/+;p53R172H/+;PdxCretg/+) mice (64, 65), harboring conditional mutations in both *Kras* and *Trp53* (gift of M. Philips, New York University, New York, New York, USA), and PDX1-Cre;Kras^{G12D};Ink4a/Arf$^{fl/fl}$ mice (66), with Kras^{G12D} expression in combination with Ink4a/Arf deficiency (gift of G. David, New York University, New York, New York, USA), were used in selected experiments. Animals were housed in a clean vivarium and fed standard mouse chow.

In vivo experiments. In vivo TLR7 ligation was accomplished by thrice-weekly i.p. administration of selective TLR7 agonists (ssRNA40, *E. coli* RNA, or Adenine analog, all 100 μg/kg; Invivogen). In selected experiments, mice were treated with the TLR2 ligand HKLM (3×10^8 cells) using the same dosing regimen. TLR7 blockade was accomplished using an oligonucleotide inhibitor of TLR7 (22) (IRS661, 100 μg every 48 hours; TIB Molbiol). Bone marrow chimeric animals were created by irradiating mice (9 Gy) followed by i.v. bone marrow transfer (1×10^7 cells) from nonirradiated donors as we previously described (67). Chimeric mice were used in experiments 7 weeks later. To accelerate carcinogenesis in p48Cre;Kras^{G12D} mice, 4 doses of caerulein (50 μg/kg) were administered over 72 hours, as described previously (21), with modifications. MAP kinase signaling blockade was accomplished using the MKK inhibitor PD98059 (2.5 mg/kg/d), and NF-κB signaling blockade was accomplished using the NEMO binding domain inhibitor (1 mg/kg/d; EMD4Biosciences). To study pancreatic inflammation in the absence of oncogenic *Kras*, chronic pancreatitis was induced in WT mice using a regimen of 7 hourly i.p. injections of caerulein (50 μg/kg; Sigma-Aldrich) thrice weekly for 3–4 weeks. For acute pancreatitis, mice were treated with 7 hourly i.p. injections of caerulein (50 μg/kg) for 2–4 consecutive days. Alternatively, twice-daily administration of L-arginine (4 g/kg; Sigma-Aldrich) for 2 days was used to induce mild acute pancreatic injury, as we described previously (67), with dose modifications.

Cellular isolation and analysis. To isolate mononuclear cells from the pancreas or spleen, organs were harvested via postmortem laparotomy and processed using both mechanical and enzymatic digestion with Collagenase IV (Sigma-Aldrich), as we described previously (67, 68). Cell surface marker analysis was performed by flow cytometry using the FACS Calibur (Beckman Coulter) after incubating 5×10^5 cells with 1 μg of anti-FcγRIII/II antibody (2.4G2, Fc block; Monoclonal Antibody Core Facility, Sloan-Kettering Institute) and then labeling with 1 μg of FITC-, PE-, PerCP-, or APC-conjugated antibodies directed against B220 (RA3-6B2), CD3ε (17A2), CD4 (RM4-5), CD8α (53–6.7), CD11b (M1/70), CD11c (HL3), CD19 (1D3), CD34 (4H11), CD45 (30-F11), CD133 (315-2C11), CD146 (P1H12), F4/80 (BM8), and Gr1 (RB6-8C5) (all eBiosciences or BioLegend). Gating strategies for leukocyte subsets was as described previously (67–69). To determine TLR7 expression, cells were fixed, permeabilized, and stained using an mAb directed against TLR7 (IMG-581A; Imgenex). In additional experiments, pancreatic mononuclear cells were stained using antibodies directed against p27 (C-19), SHPTP1 (C-19), IκB-α (H-4), Notch1 (D-11), Jagged 1 (H-66), and Delta 4 (C-20; all Santa Cruz Biotechnology), IKKα (2682; Cell Signaling), and NF-κB (ab7970; Abcam). Dead cells were identified and excluded from analysis by staining with 7-amino-actinomycin D (7AAD). Isolation and culture of PDECs from p48Cre;Kras^{G12D} mice was performed as we described previously (70, 71). In selected experiments, PDECs from

p48Cre;Kras^{G12D} mice were cultured for 72 hours alone or with ssRNA40 (2 μg/ml). Proliferation was measured by pulsing with 1 μCi [^{3}H]-thymidine for the final 24 hours. Cytokine levels in cell culture supernatant were determined using a cytometric bead array (BD Biosciences) and a MILLIPLEX MAP kit (Millipore) according to the respective manufacturers' protocols.

Western blotting. Western blotting was performed as described previously (67). Briefly, mouse pancreata or isolated PDECs were homogenized in RIPA buffer with Complete Protease Inhibitor cocktail (Roche), and proteins were separated from larger fragments by centrifugation at 14,000 *g*. Total protein concentration was determined using the BCA protein assay reagent (Thermo Scientific), according to the manufacturer's instructions. Next, 10% Bis-Tris polyacrylamide gels (NuPage; Invitrogen) were equiloaded with samples, electrophoresed at 200 V, and electrotransferred to PVDF membranes. After blocking with 5% BSA, membranes were probed with primary antibodies to Notch1 (D-11), Notch2 (ab72803), Erk1 (M233), β-actin (ab8227-50), NF-κB p65 (ab7970), p16/INK4A (2D9A12), and p-p27 (EP233[2]Y) (all Abcam); Jagged1 (H-66), Hes1 (H-140), Hey1 (W-23), PTEN (N-19), SHPTP1 (C-19), p27 (C-19), c-Myc (A-14), cyclin B1 (GNS1), cyclin D1 (M-20), Rb (C-15), IκB-α (H-4), p–IκB-α (B-9), and GAPDH (V-18) (all Santa Cruz Biotechnology); Survivin (71G4B7), CDK4 (DCS156), p–NF-κB (Ser468), p21 (DCS60), p-Akt (T308), p-Erk1 (Thr202/Tyr204), Bcl-X$_L$ (2762), STAT3 (9132), and p-STAT3 (Tyr705) (D3A7) (all Cell Signaling); p53 (CM5; Leica Microsystems); and TGF-β (1D11; R&D Systems). The HRP-conjugated secondary antibodies used were from Santa Cruz Biotechnology. Blots were developed by ECL (Thermo Scientific).

Histology, immunohistochemistry, and microscopy. For histological analysis, pancreatic specimens were fixed with 10% buffered formalin, dehydrated in ethanol, embedded with paraffin, and stained with H&E or Gomori's trichrome. Immunohistochemistry was performed using antibodies directed against B220 (BD Biosciences), CD3 (Invitrogen), p16/INK4A (Abcam), p53 (Novocastra), CK19 (University of Iowa Developmental Studies Hybridoma Bank), CD45 (BD Biosciences), α-SMA (Novus Biologicals), Erk1/2 (Santa Cruz), p-Erk1/2 (Cell Signaling), insulin (Abcam), myeloperoxidase (Lifespan Biosciences), Ki67 (Thermo Fischer Scientific), p-STAT3 (Cell Signaling), TLR2, and TLR7 (Imgenex). Light microscopic photographs were taken with a Leica DM2M microscope (Leica Microsystems) and an Optronics digital camera (Optronics). Confocal microscopy was performed on frozen pancreatic sections using Zeiss Axioskop 2 (Carl Zeiss). PanIN lesions were graded using previously established criteria (72). Quantifications were performed by examining 10 high-power fields (HPFs) per pancreas, as described previously (67). The percentage of Ki67$^+$ ductal cells as a fraction of all ductal cells was determined by manual count.

Human specimens. Deidentified paraffin-embedded tissue from 5 human resected acute pancreatitis specimens, 5 normal human pancreata, and 19 pancreatic cancer specimens were analyzed for TLR7 expression using immunohistochemistry, and the number of TLR7$^+$ cells per HPF was determined in 10 HPFs per specimen. In addition, a tissue microarray was constructed using paraffin-embedded cores from an additional 20 consecutive patients with pancreatic cancer, 10 normal pancreata, and tissue from an additional 10 patients with preinvasive PanIN lesions by examining 5 HPFs per tissue core. The percentage of TLR7$^+$ cells as a fraction of all cells was determined.

Statistics. Data are presented as mean ± SEM. Statistical significance was determined by 2-tailed Student's *t* test and/or log-rank test using GraphPad Prism 5 (GraphPad Software). *P* values less than 0.05 were considered significant.

Study approval. All human tissues were collected using a protocol approved by the New York University School of Medicine Institutional Review Board. All animal procedures were approved by the New York University School of Medicine Institutional Animal Care and Use Committee.

Acknowledgments

This work was supported by grants from the National Pancreas Foundation (to G. Miller) and by NIH awards DK085278 (to G. Miller) and CA155649 (to G. Miller).

Received for publication February 28, 2012, and accepted in revised form August 2, 2012.

Address correspondence to: George Miller, Departments of Surgery and Cell Biology, New York University School of Medicine, Medical Science Building 601, 550 First Avenue, New York, New York 10016, USA. Phone: 212.263.0570; Fax: 212.263.6840; E-mail: george.miller@nyumc.org.

1. Kuhn Y, Koscielny A, Glowka T, Hirner A, Kalff JC, Standop J. Postresection survival outcomes of pancreatic cancer according to demographic factors and socio-economic status. *Eur J Surg Oncol*. 2010; 36(5):496–500.
2. Korc M. Pancreatic cancer-associated stroma production. *Am J Surg*. 2007;194(4 suppl):S84–S86.
3. Miyamoto H, Murakami T, Tsuchida K, Sugino H, Miyake H, Tashiro S. Tumor-stroma interaction of human pancreatic cancer: acquired resistance to anticancer drugs and proliferation regulation is dependent on extracellular matrix proteins. *Pancreas*. 2004;28(1):38–44.
4. De Wever O, Mareel M. Role of tissue stroma in cancer cell invasion. *J Pathol*. 2003;200(4):429–447.
5. Ding K, Lopez-Burks M, Sanchez-Duran JA, Korc M, Lander AD. Growth factor-induced shedding of syndecan-1 confers glypican-1 dependence on mitogenic responses of cancer cells. *J Cell Biol*. 2005; 171(4):729–738.
6. Kleeff J, et al. The cell-surface heparan sulfate proteoglycan glypican-1 regulates growth factor action in pancreatic carcinoma cells and is overexpressed in human pancreatic cancer. *J Clin Invest*. 1998;102(9):1662–1673.
7. Hwang RF, et al. Cancer-associated stromal fibroblasts promote pancreatic tumor progression. *Cancer Res*. 2008;68(3):918–926.
8. Neesse A, et al. Stromal biology and therapy in pancreatic cancer. *Gut*. 2011;60(6):861–868.
9. Huang B, Zhao J, Unkeless JC, Feng ZH, Xiong H. TLR signaling by tumor and immune cells: a double-edged sword. *Oncogene*. 2008;27(2):218–224.
10. Rakoff-Nahoum S, Medzhitov R. Toll-like receptors and cancer. *Nat Rev Cancer*. 2009;9(1):57–63.
11. Lund JM, et al. Recognition of single-stranded RNA viruses by Toll-like receptor 7. *Proc Natl Acad Sci U S A*. 2004;101(15):5598–5603.
12. Doyle SL, O'Neill LA. Toll-like receptors: from the discovery of NFkappaB to new insights into transcriptional regulations in innate immunity. *Biochem Pharmacol*. 2006;72(9):1102–1113.
13. Kanzler H, Barrat FJ, Hessel EM, Coffman RL. Therapeutic targeting of innate immunity with Toll-like receptor agonists and antagonists. *Nat Med*. 2007;13(5):552–559.
14. Oshima Y, Suzuki A, Kawashimo K, Ishikawa M, Ohkohchi N, Taniguchi H. Isolation of mouse pancreatic ductal progenitor cells expressing CD133 and c-Met by flow cytometric cell sorting. *Gastroenterology*. 2007;132(2):720–732.
15. Schrage A, et al. Murine CD146 is widely expressed on endothelial cells and is recognized by the monoclonal antibody ME-9F1. *Histochem Cell Biol*. 2008; 129(4):441–451.
16. Chow JY, Quach KT, Cabrera BL, Cabral JA, Beck SE, Carethers JM. RAS/ERK modulates TGFbeta-regulated PTEN expression in human pancreatic adenocarcinoma cells. *Carcinogenesis*. 2007;28(11):2321–2327.
17. Connolly MK, et al. In hepatic fibrosis, liver sinusoidal endothelial cells acquire enhanced immunogenicity. *J Immunol*. 2010;185(4):2200–2208.
18. Fukuda A, et al. Stat3 and MMP7 contribute to pancreatic ductal adenocarcinoma initiation and progression. *Cancer Cell*. 2011;19(4):441–455.
19. Lesina M, et al. Stat3/Socs3 activation by IL-6 transsignaling promotes progression of pancreatic intraepithelial neoplasia and development of pancreatic cancer. *Cancer Cell*. 2011;19(4):456–469.
20. Yu H, Pardoll D, Jove R. STATs in cancer inflammation and immunity: a leading role for STAT3. *Nat Rev Cancer*. 2009;9(11):798–809.
21. Carriere C, Young AL, Gunn JR, Longnecker DS, Korc M. Acute pancreatitis markedly accelerates pancreatic cancer progression in mice expressing oncogenic Kras. *Biochem Biophys Res Commun*. 2009; 382(3):561–565.
22. Guiducci C, et al. Autoimmune skin inflammation is dependent on plasmacytoid dendritic cell activation by nucleic acids via TLR7 and TLR9. *J Exp Med*. 2010;207(13):2931–2942.
23. Omary MB, Lugea A, Lowe AW, Pandol SJ. The pancreatic stellate cell: a star on the rise in pancreatic diseases. *J Clin Invest*. 2007;117(1):50–59.
24. De La OJ, et al. Notch and Kras reprogram pancreatic acinar cells to ductal intraepithelial neoplasia.

Proc Natl Acad Sci U S A. 2008;105(48):18907–18912.
25. Gungor C, et al. Notch signaling activated by replication stress-induced expression of midkine drives epithelial-mesenchymal transition and chemoresistance in pancreatic cancer. *Cancer Res*. 2011; 71(14):5009–5019.
26. Hu X, et al. Integrated regulation of Toll-like receptor responses by Notch and interferon-gamma pathways. *Immunity*. 2008;29(5):691–703.
27. Maniati E, et al. Crosstalk between the canonical NF-kappaB and Notch signaling pathways inhibits Ppargamma expression and promotes pancreatic cancer progression in mice. *J Clin Invest*. 2011; 121(12):4685–4699.
28. Osipo C, Golde TE, Osborne BA, Miele LA. Off the beaten pathway: the complex cross talk between Notch and NF-kappaB. *Lab Invest*. 2008;88(1):11–17.
29. Hill R, et al. PTEN loss accelerates KrasG12D-induced pancreatic cancer development. *Cancer Res*. 2010;70(18):7114–7124.
30. Wen S, et al. PTEN controls tumor-induced angiogenesis. *Proc Natl Acad Sci U S A*. 2001;98(8):4622–4627.
31. Nagy A, et al. Copy number of cancer genes predict tumor grade and survival of pancreatic cancer patients. *Anticancer Res*. 2001;21(2B):1321–1325.
32. Plath T, et al. Overexpression of pRB in human pancreatic carcinoma cells: function in chemotherapy-induced apoptosis. *J Natl Cancer Inst*. 2002; 94(2):129–142.
33. Rosty C, et al. p16 Inactivation in pancreatic intraepithelial neoplasias (PanINs) arising in patients with chronic pancreatitis. *Am J Surg Pathol*. 2003; 27(12):1495–1501.
34. Carriere C, et al. Deletion of Rb accelerates pancreatic carcinogenesis by oncogenic Kras and impairs senescence in premalignant lesions. *Gastroenterology*. 2011;141(3):1091–1101.
35. Takaoka A, et al. Integration of interferon-alpha/beta signalling to p53 responses in tumour suppression and antiviral defence. *Nature*. 2003; 424(6948):516–523.
36. Ide T, et al. Tumor-stromal cell interaction under hypoxia increases the invasiveness of pancreatic cancer cells through the hepatocyte growth factor/c-Met pathway. *Int J Cancer*. 2006;119(12):2750–2759.
37. Chu GC, Kimmelman AC, Hezel AF, DePinho RA. Stromal biology of pancreatic cancer. *J Cell Biochem*. 2007;101(4):887–907.
38. Andersson ER, Sandberg R, Lendahl U. Notch signaling: simplicity in design, versatility in function. *Development*. 2011;138(17):3593–3612.
39. Salaun B, Coste I, Rissoan MC, Lebecque SJ, Renno T. TLR3 can directly trigger apoptosis in human cancer cells. *J Immunol*. 2006;176(8):4894–4901.
40. Sfondrini L, et al. Antitumor activity of the TLR-5 ligand flagellin in mouse models of cancer. *J Immunol*. 2006;176(11):6624–6630.
41. Spaner DE, Masellis A. Toll-like receptor agonists in the treatment of chronic lymphocytic leukemia. *Leukemia*. 2007;21(1):53–60.
42. Gauvreau GM, Hessel EM, Boulet LP, Coffman RL, O'Byrne PM. Immunostimulatory sequences regulate interferon-inducible genes but not allergic airway responses. *Am J Respir Crit Care Med*. 2006; 174(1):15–20.
43. Butts C, et al. Randomized phase IIB trial of BLP25 liposome vaccine in stage IIIB and IV non-small-cell lung cancer. *J Clin Oncol*. 2005;23(27):6674–6681.
44. Roses RE, Xu M, Koski GK, Czerniecki BJ. Radiation therapy and Toll-like receptor signaling: implications for the treatment of cancer. *Oncogene*. 2008; 27(2):200–207.
45. Wang RF, Miyahara Y, Wang HY. Toll-like receptors and immune regulation: implications for cancer therapy. *Oncogene*. 2008;27(2):181–189.
46. Chen K, Huang J, Gong W, Iribarren P, Dunlop NM, Wang JM. Toll-like receptors in inflammation, infection and cancer. *Int Immunopharmacol*. 2007; 7(10):1271–1285.
47. Lu H, et al. Treatment failure of a TLR-7 agonist occurs due to self-regulation of acute inflammation and can be overcome by IL-10 blockade. *J Immunol*. 2010;184(9):5360–5367.
48. Fukata M, Abreu MT. Role of Toll-like receptors in gastrointestinal malignancies. *Oncogene*. 2008; 27(2):234–243.
49. Fukata M, et al. Toll-like receptor-4 promotes the development of colitis-associated colorectal tumors. *Gastroenterology*. 2007;133(6):1869–1881.
50. Lowenfels AB, et al. Hereditary pancreatitis and the risk of pancreatic cancer. International Hereditary Pancreatitis Study Group. *J Natl Cancer Inst*. 1997; 89(6):442–446.
51. Lowenfels AB, et al. Pancreatitis and the risk of pancreatic cancer. International Pancreatitis Study Group. *N Engl J Med*. 1993;328(20):1433–1437.
52. Grimm M, et al. Toll-like receptor (TLR) 7 and TLR8 expression on CD133+ cells in colorectal cancer points to a specific role for inflammation-induced TLRs in tumourigenesis and tumour progression. *Eur J Cancer*. 2010;46(15):2849–2857.
53. Cherfils-Vicini J, et al. Triggering of TLR7 and TLR8 expressed by human lung cancer cells induces cell survival and chemoresistance. *J Clin Invest*. 2010; 120(4):1285–1297.
54. Gress TM, et al. Differential expression of heat shock proteins in pancreatic carcinoma. *Cancer Res*. 1994;54(2):547–551.
55. Sato Y, Goto Y, Narita N, Hoon DS. Cancer cells expressing toll-like receptors and the tumor microenvironment. *Cancer Microenviron*. 2009; 2(suppl 1):205–214.
56. Tang D, Loze MT, Zeh HJ, Kang R. The redox protein HMGB1 regulates cell death and survival in cancer treatment. *Autophagy*. 2010;6(8):1181–1183.
57. Heil F, et al. Species-specific recognition of single-stranded RNA via toll-like receptor 7 and 8. *Science*. 2004;303(5663):1526–1529.
58. Tomasiewicz K, Modrzewska R, Lyczak A, Krawczuk G. TT virus infection and pancreatic cancer: relationship or accidental coexistence. *World J Gastroenterol*. 2005;11(18):2847–2849.
59. Hassan MM, et al. Association between hepatitis B virus and pancreatic cancer. *J Clin Oncol*. 2008; 26(28):4557–4562.
60. Di Bisceglie AM. Hepatitis C and hepatocellular carcinoma. *Hepatology*. 1997;26(3 suppl 1):34S–38S.
61. De Mitri MS, et al. HCV-associated liver cancer without cirrhosis. *Lancet*. 1995;345(8947):413–415.
62. El-Serag HB, et al. Risk of hepatobiliary and pancreatic cancers after hepatitis C virus infection: A population-based study of U.S. veterans. *Hepatology*. 2009;49(1):116–123.
63. Tuveson DA, et al. Endogenous oncogenic K-ras(G12D) stimulates proliferation and widespread neoplastic and developmental defects. *Cancer Cell*. 2004;5(4):375–387.
64. Hingorani SR, et al. Trp53R172H and KrasG12D cooperate to promote chromosomal instability and widely metastatic pancreatic ductal adenocarcinoma in mice. *Cancer Cell*. 2005;7(5):469–483.
65. Olive KP, et al. Inhibition of Hedgehog signaling enhances delivery of chemotherapy in a mouse model of pancreatic cancer. *Science*. 2009; 324(5933):1457–1461.
66. Aguirre AJ, et al. Activated Kras and Ink4a/Arf deficiency cooperate to produce metastatic pancreatic ductal adenocarcinoma. *Genes Development*. 2003;17(24):3112–3126.
67. Bedrosian AS, et al. Dendritic cells promote pancreatic viability in mice with acute pancreatitis. *Gastroenterology*. 2011;141(5):1915–1926.
68. Connolly MK, et al. In liver fibrosis, dendritic cells govern hepatic inflammation in mice via TNF-alpha. *J Clin Invest*. 2009;119(11):3213–3225.
69. Connolly MK, et al. Distinct populations of metastases-enabling myeloid cells expand in the liver of mice harboring invasive and preinvasive intra-abdominal tumor. *J Leukoc Biol*. 2010;87(4):713–725.
70. Pylayeva-Gupta Y, Lee KE, Hajdu CH, Miller G, Bar-Sagi D. Oncogenic Kras-induced GM-CSF production promotes the development of pancreatic neoplasia. *Cancer Cell*. 2012;21(6):836–847.
71. Agbunag C, Lee KE, Buontempo S, Bar-Sagi D. Pancreatic duct epithelial cell isolation and cultivation in two-dimensional and three-dimensional culture systems. *Methods Enzymol*. 2006;407:703–710.
72. Hruban RH, et al. An illustrated consensus on the classification of pancreatic intraepithelial neoplasia and intraductal papillary mucinous neoplasms. *Am J Surg Pathol*. 2004;28(8):977–987.